

Two-Dimensional Spectra in the Atmospheric Boundary Layer

MARK KELLY

Department of Meteorology, The Pennsylvania State University, University Park, Pennsylvania

JOHN C. WYNGAARD

Department of Meteorology, and Department of Mechanical Engineering, The Pennsylvania State University, University Park, Pennsylvania

(Manuscript received 22 August 2005, in final form 25 January 2006)

ABSTRACT

One-dimensional spectra are frequently used to relate features of measured and simulated meteorological field variables in the turbulent atmospheric boundary layer (ABL), but two-dimensional spectra can provide more reliable scale information than one-dimensional spectra. Here a method is presented for obtaining two-dimensional spectra from one-dimensional spectra, and it includes examples using data from large-eddy simulations and field measurements in the ABL.

1. Introduction

The one-dimensional spectrum is the most commonly used type in atmospheric boundary layer (ABL) studies. Time series of meteorological variables are readily transformed into frequency spectra via discrete Fourier transform, and these spectra are in turn converted into streamwise wavenumber spectra through Taylor's hypothesis ($\partial/\partial t \approx -U\partial/\partial x$). But by definition one-dimensional spectra become constant as wavenumber (frequency) approaches zero. Specifically, the one-dimensional spectrum $F_c(\kappa_1)$ of a fluctuating variable $c(x)$ has a value at zero wavenumber, which is proportional to the integral scale \mathcal{L}_c .¹

$$F_c(0) = \frac{2}{\pi} \int_0^\infty \overline{c(x)c(x+\xi)} d\xi = \frac{2}{\pi} \mathcal{L}_c \overline{c^2}, \quad (1)$$

where the integral scale is defined by

¹ The relation (1) follows from defining $F_c(\kappa_1)$ as the Fourier transform of the autocovariance $\overline{c(x)c(x+\xi)}$ (and vice versa), $F_c(\kappa_1) = (2/\pi) \int_0^\infty \overline{c(x)c(x+\xi)} e^{i\kappa_1 \xi} d\xi$.

Corresponding author address: Mark Kelly, The Pennsylvania State University, 503 Walker Building, University Park, PA 16802.
E-mail: MCK154@psu.edu

$$\mathcal{L}_c \equiv \frac{1}{c^2} \int_0^\infty \overline{c(x)c(x+\xi)} d\xi \quad (2)$$

and overbars indicate an average over the entire spatial record of $c(x)$. In addition, modes traveling nearly perpendicular to the streamwise direction appear to be of very low wavenumber (Tennekes and Lumley 1972, section 8.1). Thus the one-dimensional spectrum does not represent spectral peaks and associated spatial-scale information reliably.

Both the classical three-dimensional spectrum (Batchelor 1953) and its counterpart in the plane, the two-dimensional spectrum (Peltier et al. 1996), vanish at zero wavenumber; this is consistent with the absence of turbulent kinetic energy or scalar variance there. By their nature they convey scale information better than one-dimensional spectra. Until recently they were essentially unmeasurable in the ABL, but arrays of meteorological sensors (Tong et al. 1998; Sullivan et al. 2003) as well as computer simulations (Peltier et al. 1996; Wijesekera et al. 2004) now make them accessible. This note presents a method for calculating two-dimensional spectra from one-dimensional streamwise spectra, using the assumption of axisymmetry (isotropy in the horizontal plane). We provide several examples based on data from large-eddy simulation and aircraft measurements.

2. One- and two-dimensional spectra

The atmospheric boundary layer is inhomogeneous in the vertical, but can be homogeneous in the horizontal plane. For that reason Peltier et al. (1996) suggested calculating spectra in that plane rather than along horizontal lines, as had been traditional. Thus, following Peltier et al. we denote the power spectral density of a scalar $c(x, y, z; t)$ at height z in the homogeneous horizontal plane as $\psi_c(\boldsymbol{\kappa}_h; z; t)$, where $\boldsymbol{\kappa}_h \equiv (\kappa_1, \kappa_2)$. It integrates over the horizontal wavenumber plane to the variance:

$$\iint_{-\infty}^{\infty} \psi_c(\boldsymbol{\kappa}_h) d\kappa_1 d\kappa_2 = \overline{c^2}$$

(for the sake of simplicity, we shall hereafter suppress dependencies upon z and t). The streamwise one-dimensional wavenumber spectrum $F_c(\kappa_1)$ is related to $\psi_c(\boldsymbol{\kappa}_h)$ by

$$F_c(\kappa_1) = \int_{-\infty}^{\infty} \psi_c(\kappa_1, \kappa_2) d\kappa_2. \quad (3)$$

In the ABL, velocity and scalar fields can approach isotropy in the horizontal plane as the flow approaches free convection. Under the assumption of such isotropy, also called axisymmetry (Batchelor 1953), the power spectral density depends only on horizontal wavenumber magnitude κ_h . Thus in analogy to the classical three-dimensional spectrum, Peltier et al. (1996) defined a two-dimensional spectrum $E_c(\boldsymbol{\kappa}_h)$ by integrating $\psi_c(\boldsymbol{\kappa}_h)$ over circular rings of radius κ_h :

$$E_c(\boldsymbol{\kappa}_h) = \int_0^{2\pi} \psi_c(\boldsymbol{\kappa}_h) \kappa_h d\theta = 2\pi \kappa_h \psi_c(\boldsymbol{\kappa}_h). \quad (4)$$

It integrates over its argument to the variance,

$$\int_0^{\infty} E_c(\boldsymbol{\kappa}_h) d\kappa_h = \overline{c^2}.$$

Through $\psi_c(\boldsymbol{\kappa}_h)$ we relate the one-dimensional spectrum F_c to the two-dimensional spectrum E_c ; from Eqs. (3) and (4) we see that

$$F_c(\kappa_1) = \int_{-\infty}^{\infty} \frac{E_c(\boldsymbol{\kappa}_h)}{2\pi(\kappa_1^2 + \kappa_2^2)^{1/2}} d\kappa_2. \quad (5)$$

Unlike the case for three-dimensional spectra, which are related under isotropy to one-dimensional spectra through a simple differential equation, there is no closed differential expression relating $E_c(\boldsymbol{\kappa}_h)$ to $F_c(\kappa_1)$. It is possible, however, to invert (5), which produces

$$E_c(\boldsymbol{\kappa}_h) = -\frac{d}{d\kappa_h} \int_{\kappa_h}^{\infty} \frac{2\kappa_1 F_c(\kappa_1)}{(\kappa_1^2 - \kappa_h^2)^{1/2}} d\kappa_1. \quad (6)$$

The apparent singularity in $E_c(\boldsymbol{\kappa}_h)$ is merely an artifact of the analytic form in which it is presented. For example, if $F_c(\kappa_1) \propto \kappa_1^{-5/3}$, the integral in (6) evaluated at κ_h is finite. A detailed derivation of (6) is included in the appendix.

3. Two-dimensional spectra from measured fields and simulations

In the atmospheric boundary layer the fluctuating vertical velocity w is a scalar on the horizontal plane. Assuming isotropy in the plane, the two-dimensional spectrum of $w(x, y)$ depends solely upon horizontal wavenumber magnitude κ_h . In this section we calculate the two-dimensional spectrum of vertical velocity fluctuations, using data from both large-eddy simulation and measurements in the atmospheric boundary layer.

a. Spectra calculated from large-eddy simulation

The large-eddy simulation (LES) data used here include three-dimensional velocity and scalar fields, allowing computation of the spectral density and thus facilitating direct calculation of both one- and two-dimensional spectra. We use a $5 \times 5 \times 1.5 \text{ km}^3$, $400 \times 400 \times 96$ point section of data from simulation of a convective ABL (P. Sullivan 2004, personal communication). Here we consider the vertical velocity field $w(x, y)$ from the sixth grid level, close enough to the lower boundary for the vertical velocity to scale with z but sufficiently high to avoid surface-induced horizontal anisotropy or excessive influence of the simulation's sub-filter models. The power spectral density of vertical velocity fluctuations $\phi_{33}(\kappa_1, \kappa_2)$ is calculated by fast-Fourier transform, then used in (3) and (4) to obtain the one- and two-dimensional spectra $F_v(\kappa_1)$ and $E_v(\boldsymbol{\kappa}_h)$; the spectrum $E_v(\boldsymbol{\kappa}_h)$ is also computed from $F_v(\kappa_1)$ via (6). Here we use subscript v to denote vertical (velocity), as in Peltier et al. (1996).

Figure 1 displays $E_v(\boldsymbol{\kappa}_h)$ and $F_v(\kappa_1)$. As expected, $E_v(\boldsymbol{\kappa}_h)$ goes to zero at small wavenumbers, whereas $F_v(\kappa_1)$ becomes constant as $\kappa_1 \rightarrow 0$. The figure also includes the so-called pre-multiplied spectrum $\kappa_1 F_v(\kappa_1)$, which vanishes as $\kappa_1 \rightarrow 0$ and appears to have features similar to $E_v(\boldsymbol{\kappa}_h)$. The common practice of plotting pre-multiplied one-dimensional spectra² can be misleading,

² The practice of plotting one-dimensional spectra multiplied by wavenumber stems from the equality $\int F(\kappa_1) d\kappa_1 = \int \kappa_1 F(\kappa_1) d \log \kappa_1$; i.e. a plot of $\kappa_1 F(\kappa_1)$ versus $\log \kappa_1$ is variance preserving.

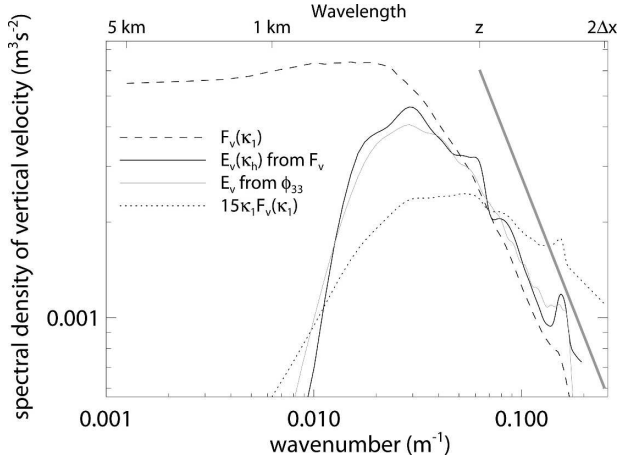


FIG. 1. Two-dimensional spectrum $E_v(\kappa_h)$ and streamwise one-dimensional spectrum $F_v(\kappa_1)$ of vertical velocity, from LES at height $z \sim 0.07z_t$. Dashed line is $F_v(\kappa_1)$, solid line is $E_v(\kappa_h)$ computed from $F_v(\kappa_1)$ using (6), light solid line is $E_v(\kappa_h)$ calculated directly from $\phi_{33}(\kappa_h)$ via (4), and dotted line is $\kappa_1 F_v(\kappa_1)$ (multiplied by a factor of 15 to appear on same plot). Thick straight line is Kolmogorov ($-5/3$) power law.

however. Plots of $\kappa_1 F(\kappa_1)$ can exhibit peaks at scales different than those representative of the physical processes that generate variance (Tennekes and Lumley 1972), and these peaks are often broad or even indiscernible. For example, $E_v(\kappa_h)$ in Fig. 1 has its peak around 0.03 m^{-1} but $\kappa_1 F_v(\kappa_1)$ has a wider and less defined peak somewhere between 0.03 m^{-1} and $\sim 2\pi/z$. Comparing $\kappa_1 F_v(\kappa_1)$ to $E_v(\kappa_h)$, the figure demonstrates that the one-dimensional spectrum is a “smeared” form of the two-dimensional spectrum—analogue to the relationship between two- and three-dimensional spectra (Peacock 1999, section 18.1). Thus $E_v(\kappa_h)$ displays more clearly the features of $w(x, y)$ than does $\kappa_1 F_v(\kappa_1)$, despite containing less information due to the limits of resolution and the numerical implementation of (6).

Finally, Fig. 1 shows that the inversion (6) gives reasonably accurate results, considering we used simple first-order differences and Simpson’s rule to calculate the two-dimensional spectra: $E_v(\kappa_h)$ calculated from $F_v(\kappa_1)$ agrees rather well with $E_v(\kappa_h)$ calculated directly from the power spectral density $\phi_{33}(\kappa_1, \kappa_2)$. All spectra were smoothed in order to display them more clearly and to reduce the amount of high-wavenumber noise input into (6), because the inversion is sensitive to variations $dF/d\kappa_1$. The velocity spectra we present here are realistic, as our plots of $\kappa_1 F(\kappa_1)$ are consistent with the universal log–log plots of Kaimal et al. (1976).

b. Spectra calculated from atmospheric measurements

As an example of obtaining two-dimensional spectra from time series of measured fields, we use velocities

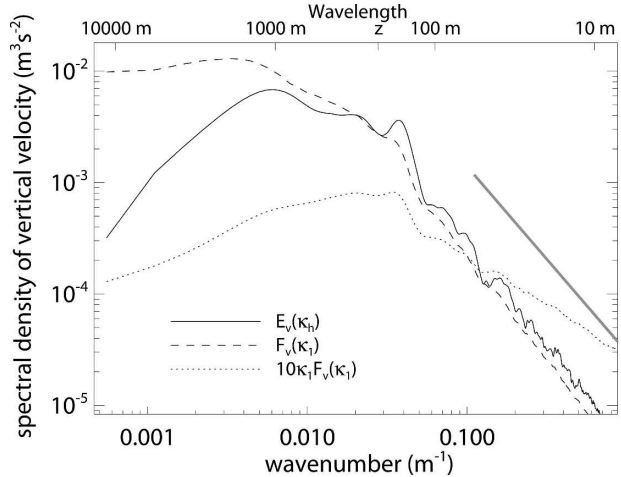


FIG. 2. Two-dimensional spectrum $E_v(\kappa_h)$ and streamwise one-dimensional spectrum $F_v(\kappa_1)$ of vertical velocity, from DYCOMS-II data. Solid line is $E_v(\kappa_h)$, dashed line is $F_v(\kappa_1)$, and dotted line is $10 \kappa_1 F_v(\kappa_1)$. Thick straight line is Kolmogorov ($-5/3$) power law.

measured by linear airplane traverse through a modestly convective atmospheric boundary layer over the ocean. The example presented here uses a 17-min segment of data from the Second Dynamics and Chemistry of Marine Stratocumulus (DYCOMS-II) experiment (Stevens et al. 2003), taken from an airplane at an altitude of 225 m over a distance of about 113 km (with rms deviations in the plane’s velocity and altitude of $\sim 1\%$), sampled at 25 Hz. Taylor’s hypothesis and the speed of the airplane are used to convert the measured time series into a spatial record.

Figure 2 shows the one-dimensional spectrum of vertical velocity fluctuations calculated from the DYCOMS-II data, and the two-dimensional spectrum which follows via (6). Again $E_v(\kappa_h)$ has more clearly defined features than $\kappa_1 F_v(\kappa_1)$. The two-dimensional spectrum peaks at $\kappa_h \sim 0.006 \text{ m}^{-1}$, which corresponds to turbulence at scales on the order of the boundary layer depth. Such a feature is not evident in $\kappa_1 F_v(\kappa_1)$, which exhibits a broad peak near $\kappa_1 \sim 0.033 \text{ m}^{-1}$ that is coincident with a secondary peak in $E_v(\kappa_h)$, but which roughly corresponds to the measurement altitude z —and thus may be an artifact of the measurement process. Note however that the $\kappa_1 F_v(\kappa_1)$ in Fig. 2 seems to loosely conform to the unstable boundary layer spectra given by Kaimal et al. (1976).

c. The assumption of axisymmetry

Thus far we have relied upon the assumption of horizontal isotropy (axisymmetry) to obtain two-dimensional spectra $E_v(\kappa_h)$ from one-dimensional

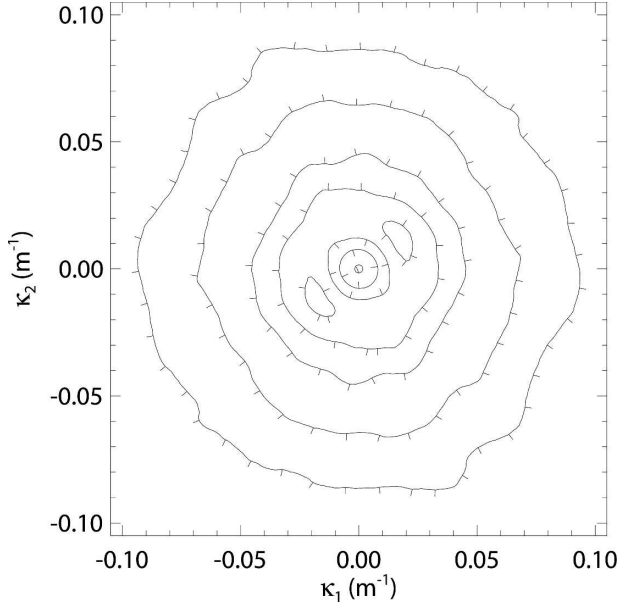


FIG. 3. Contour plot of the power spectral density $\phi_{33}(\kappa_1, \kappa_2)$ of vertical velocity taken from the LES data. Contour tick marks indicate direction of decreasing ϕ_{33} .

$F_v(\kappa_1)$. Invoking axisymmetry allows us to average the power spectral density over circular rings of radius $\kappa_h = \sqrt{\kappa_1^2 + \kappa_2^2}$ order to obtain $E_v(\kappa_h)$, through either (4) or (6). The large-eddy simulation data analyzed in section 3b were taken from a grid level where axisymmetry applies, as shown in Fig. 3.

The figure displays contours of the two-dimensional power spectral density of vertical velocity $\phi_{33}(\kappa_1, \kappa_2)$; the contours are essentially circular, particularly at larger wavenumbers. Closer to the ground, horizontal anisotropy causes the contours of $\phi_{33}(\kappa_1, \kappa_2)$ to become elliptical, compressed in the κ_1 direction. As the bottom of the ABL is approached (say for z significantly smaller than the Monin–Obukhov length), the utility of the ring average and two-dimensional spectrum is reduced, because there are different turbulence scales in the x and y directions. But for modest departures from axisymmetry, one can devise various simple means to account for elliptical contours of the power spectral density. The DYCOMS-II data analyzed likely satisfy axisymmetry as well, given that convection prevails at a measurement altitude greater than the magnitude of the Monin–Obukhov length.

4. Summary

We have devised a method to calculate two-dimensional spectra of scalar quantities in the atmospheric boundary layer under the assumption of hori-

zontal isotropy. The method is demonstrated with both measured and simulated data, which show that two-dimensional spectra contain better scale information than oft-used one-dimensional spectra. The method is adaptable to modest departures from horizontal isotropy near the surface, and is computationally simple to implement.

Acknowledgments. We thank Peter Sullivan for the large-eddy simulation data, and Donald Lenschow for guidance regarding access to and use of the DYCOMS-II boundary layer flight data. This work was supported in part by AASERT Grant DAAG55-98-1-0189 and NSF Award 0349410.

APPENDIX

Obtaining $E_c(\kappa_h)$ from $F_c(\kappa_1)$

We need to invert the relation (5) in order to get $E_c(\kappa_h)$ in terms of $F_c(\kappa_1)$. Upon recognizing that $\kappa_2^2 = \kappa_h^2 - \kappa_1^2$, so that $d\kappa_2/\kappa_h = d\kappa_h/\kappa_2$, Eq. (5) becomes

$$F_c(\kappa_1) = \int_{\kappa_1}^{\infty} \frac{E_c(\kappa_h) d\kappa_h}{2\pi(\kappa_h^2 - \kappa_1^2)^{1/2}}. \quad (\text{A1})$$

Equation (A1) is an integral of the Abel-like form (Estrada and Kanwal 2000)

$$f(s) = \int_s^{\infty} \frac{g(t) dt}{[h(t) - h(s)]^\alpha}, \quad 0 < \alpha < 1 \quad (\text{A2})$$

where $(s, t) = (\kappa_1, \kappa_h)$, $f(s) = F_c(\kappa_1)$, $g(t) = E_c(\kappa_h)/2\pi$, $h(t) = \kappa_h^2$, and $\alpha = 1/2$. Since h is a strictly increasing differentiable function, we may substitute $f(u)$ from (A2) into

$$\int_s^{\infty} \frac{h'(u)f(u) du}{[h(u) - h(s)]^{1-\alpha}}$$

to get

$$\int_s^{\infty} \int_u^{\infty} \frac{-g(t)dt h'(u) du}{[h(u) - h(t)]^\alpha [h(s) - h(u)]^{1-\alpha}}, \quad (\text{A3})$$

where primes denote derivative with respect to the argument. Changing the order of integration, (A3) becomes

$$\frac{-\pi}{\sin(\alpha\pi)} \int_s^{\infty} g(t) dt. \quad (\text{A4})$$

Then

$$\begin{aligned} \frac{d}{dt} \int_s^{\infty} \frac{h'(u)f(u) du}{[h(s) - h(u)]^{1-\alpha}} &= \frac{d}{dt} \left[\frac{-\pi}{\sin(\alpha\pi)} \int_s^{\infty} g(t) dt \right] \\ &= \frac{-\pi}{\sin(\alpha\pi)} g(t) \end{aligned}$$

so that

$$g(t) = \frac{-\sin(\alpha\pi)}{\pi} \frac{d}{dt} \int_s^\infty \frac{h'(u)f(u) du}{[h(s) - h(u)]^{1-\alpha}}. \quad (\text{A5})$$

Plugging our variables back in for s , t , α , h , f , and g we obtain

$$E_c(\kappa_h) = -\frac{d}{d\kappa_h} \int_{\kappa_h}^\infty \frac{2uF_c(u) du}{(u^2 - \kappa_h^2)^{1/2}}. \quad (\text{A6})$$

Since u is a dummy variable and can be written as κ_1 , (A6) becomes (6).

REFERENCES

- Batchelor, G., 1953: *The Theory of Homogeneous Turbulence*. Cambridge University Press, 197 pp.
- Estrada, R., and R. Kanwal, 2000: *Singular Integral Equations*. Birkhäuser, 427 pp.
- Kaimal, J. C., J. C. Wyngaard, D. A. Haugen, O. R. Coté, Y. Izumi, S. J. Caughey, and C. J. Readings, 1976: Turbulence structure in the convective boundary layer. *J. Atmos. Sci.*, **33**, 2152–2169.
- Peacock, J. A., 1999: *Cosmological Physics*. Cambridge University Press, 682 pp.
- Peltier, L. J., J. C. Wyngaard, S. Khanna, and J. G. Brasseur, 1996: Spectra in the unstable surface layer. *J. Atmos. Sci.*, **53**, 49–61.
- Stevens, B., and Coauthors, 2003: Dynamics and chemistry of marine stratocumulus—DYCOMS-II. *Bull. Amer. Meteor. Soc.*, **84**, 579–593.
- Sullivan, P. P., T. W. Horst, D. H. Lenschow, C.-H. Moeng, and J. C. Weil, 2003: Structure of subfilter-scale fluxes in the atmospheric surface layer with application to large-eddy simulation modeling. *J. Fluid Mech.*, **482**, 101–139.
- Tennekes, H., and J. Lumley, 1972: *A First Course in Turbulence*. MIT Press, 300 pp.
- Tong, C., J. Wyngaard, S. Khanna, and J. Brasseur, 1998: Resolvable and subgrid-scale measurement in the atmospheric surface layer: Technique and issues. *J. Atmos. Sci.*, **55**, 3114–3126.
- Wijesekera, H. W., C. A. Paulson, and E. D. Skyllingstad, 2004: Scaled temperature spectrum in the unstable oceanic surface layer. *J. Geophys. Res.*, **109**, 1–11.